Received: 7 January 2023 | Accepted: 21 April 2023

DOI: 10.1002/ame2.12327

ORIGINAL ARTICLE

Perilipin 5 regulates hepatic stellate cell activation and high-fat diet-induced non-alcoholic fatty liver disease

Xuecui Yin[1] | Lin Dong[2] | Xiaohan Wang[2] | Zhenzhen Qin[1] | Yuying Ma[1] | Xiaofei Ke[2] | Ya Li[1] | Qingde Wang[1] | Yang Mi[1] | Quanjun Lyu[3] | Xia Xu[4] | Pengyuan Zheng[1] | Youcai Tang[1,5]

[1]Department of Internal Medicine, the Fifth Affiliated Hospital of Zhengzhou University, Zhengzhou, China

[2]Department of Pediatrics, the Fifth Affiliated Hospital of Zhengzhou University, Zhengzhou, China

[3]Department of Clinical Nutrition, the First Affiliated Hospital of Zhengzhou University, Zhengzhou, China

[4]Key Laboratory of Advanced Drug Preparation Technologies, Ministry of Education of China, Co-innovation Center of Henan Province for New drug R & D and Preclinical Safety, School of Pharmaceutical Sciences, Zhengzhou University, Zhengzhou, China

[5]Department of Pediatrics, Gastroenterology, Henan Key Laboratory of Rehabilitation Medicine, Henan Joint International Research Laboratory of Chronic Liver Injury and Henan Provincial Outstanding Overseas Scientists Chronic Liver Injury Studio, the Fifth Affiliated Hospital of Zhengzhou University, Zhengzhou, China

Correspondence
Youcai Tang and Pengyuan Zheng, Department of Internal Medicine, the Fifth Affiliated Hospital of Zhengzhou University, 3 Kangfuqian Street, Zhengzhou, Henan 450003, China.
Email: tangyoucai@hotmail.com and medp7123@126.com

Xia Xu, Key Laboratory of Advanced Drug Preparation Technologies, Ministry of Education of China, Co-innovation Center of Henan Province for New drug R & D and Preclinical Safety, School of Pharmaceutical Sciences, Zhengzhou University, Zhengzhou, Henan 450001, China.
Email: xuxia@zzu.edu.cn

Funding information
Discipline Key Special Project, Grant/Award Number: XKZDQY202001; Henan Provincial Key R&D and Promotion Special Project, Grant/Award Number: 212102310033; Henan Provincial Medical Science and Technology Tackling Program, Grant/Award Number: LHGJ20220557; Key R&D Program of China, Grant/Award Number: 2020YFC2006100, 2020YFC2009000 and 2020YFC2009006; National Natural

Abstract

Background: Nonalcoholic fatty liver disease (NAFLD) is one of the most common chronic liver diseases globally. Hepatic stellate cells (HSCs) are the major effector cells of liver fibrosis. HSCs contain abundant lipid droplets (LDs) in their cytoplasm during quiescence. Perilipin 5 (PLIN 5) is a LD surface-associated protein that plays a crucial role in lipid homeostasis. However, little is known about the role of PLIN 5 in HSC activation.

Methods: PLIN 5 was overexpressed in HSCs of Sprague–Dawley rats by lentivirus transfection. At the same time, PLIN 5 gene knockout mice were constructed and fed with a high-fat diet (HFD) for 20 weeks to study the role of PLIN 5 in NAFLD. The corresponding reagent kits were used to measure TG, GSH, Caspase 3 activity, ATP level, and mitochondrial DNA copy number. Metabolomic analysis of mice liver tissue metabolism was performed based on UPLC-MS/MS. AMPK, mitochondrial function, cell proliferation, and apoptosis-related genes and proteins were detected by western blotting and qPCR.

Results: Overexpression of PLIN 5 in activated HSCs led to a decrease in ATP levels in mitochondria, inhibition of cell proliferation, and a significant increase in cell apoptosis through AMPK activation. In addition, compared with the HFD-fed C57BL/6J mice, PLIN 5 knockout mice fed with HFD showed reduced liver fat deposition, decreased LD abundance and size, and reduced liver fibrosis.

Xuecui Yin, Lin Dong, and Xiaohan Wang contributed equally to this work.

Science Foundation of China, Grant/
Award Number: 31471330 and 81870408

Conclusion: These findings highlight the unique regulatory role of PLIN 5 in HSCs and the role of PLIN 5 in the fibrosis process of NAFLD.

KEYWORDS
AMPK, apoptosis, hepatic stellate cell, liver fibrosis, perilipin 5

1 | INTRODUCTION

NAFLD is a chronic liver disease with a range spectrum from simple fatty liver to advanced non-alcoholic steatohepatitis (NASH).[1] About a third of patients develop hepatic fibrogenesis, even cirrhosis and hepatocellular carcinoma,[2] but underlying mechanisms of pathogenesis generally remain elusive.

Hepatic stellate cells (HSCs) locate between hepatocytes and sinusoidal endothelial cells and are known as the main effectors of hepatic fibrogenesis.[3] In a healthy liver, HSCs stay at a quiescent state with a large number of lipid droplets (LDs) rich in retinol.[4] During chronic liver damage, HSCs transdifferentiate into myofibroblast-like cells with concomitant loss of their LDs, de novo synthesis of α-smooth muscle actin (α-SMA) and α1 type I collagen, leading to an imbalanced formation and degradation of extracellular matrix (ECM).[4] This process is known as HSC activation, presenting a high proliferation rate and initiating liver fibrosis.[4] Although advances in the understanding of genes promoting HSC activation are impressive, there are no effective therapeutic interventions available for hepatic fibrogenesis.[5] As a consequence, inhibition or reversion of HSC activation or induction of apoptosis or necrosis of activated HSCs, could help in further understanding of hepatic fibrosis and suggest novel therapeutic strategies.

Perilipin 5 (PLIN5), also called oxidative tissue-enriched PAT protein (OXPAT) and lipid storage droplet protein 5 (LSDP5), is a newly confirmed member of the perilipin family and is highly expressed in oxidative tissues, such as the heart, brown adipocytes, skeletal muscle and liver.[6–8] PLIN5 forms a coat on the surface of LDs that store neutral lipids,[9] such as triacylglycerol (TAG) and cholesterol ester, playing a critical role in lipid homeostasis in mammalian cells.[10] LDs are found in almost all types of the cell including quiescent HSCs; however, their characteristics greatly vary in different tissues.[11] Recently, studies have confirmed that intracellular lipid contents influence the activated status of HSCs[12–15] and the functions of PLIN5 in hepatocytes,[16,17] heart,[18] skeletal muscle,[16] and islets,[19] covering lipid metabolism,[20] insulin secretion[21] and specifically regulating mitochondrial function in cardiac[18] and skeletal muscle.[16] It has been reported that PLIN5 may inhibit HSC activation[22] and little is known about the role of Plin5 in apoptosis of activated HSCs. In this study, we explored the role of PLIN 5 in HSCs, and also report the impact of PLIN 5 deletion in HFD-induced NAFLD and hepatic fibrosis in vivo.

2 | MATERIALS AND METHODS

2.1 | Animal preparations

Sprague–Dawley (SD, male, 6–8 weeks old) rats were purchased from the Henan Experimental Animal Center (Zhengzhou, China). C57BL/6J mice were obtained from Beijing HFK Bioscience (Beijing, China.) PLIN 5−/− mice were generated by the Nanjing Biomedical Research Institute of Nanjing University and identified by gene and protein expression. Four-week-old mice of each strain were randomly divided into normal diet (ND) and high-fat diet with high fructose corn syrup (HFD, 45% energy from fat, H10045; Beijing HFK Bioscience) groups, fed the respective diets for 20 weeks ($n = 10$ per group; 4 groups).[23] All the mice and rats used in this work received humane care in compliance with institutional animal care guidelines and the study was approved by the Animal Ethics Committee of Zhengzhou University (KY2022045). All protocols were conducted according to the *Guidance Suggestions for the Care and Use of Laboratory Animals*, formulated by the Ministry of Science and Technology of China.

2.2 | Isolation and culture of HSCs

HSCs were isolated by the pronase–collagenase perfusion in situ before density gradient centrifugation.[24] To obtain primary hepatic stellate cells (rHSC-primary), we isolated them from normal livers and then cultured them in low-glucose DMEM containing 10% of FBS for 24 h (called one-day cultured HSCs or D1 HSCs, which stay close to a quiescent state, thus helping to exclude non-HSC cell types), 7 days (called 7-day cultured HSCs or D7 HSCs, which are almost entirely activated) or 4–9 passages (rHSC-primary, which are fully activated). Unless otherwise mentioned, rHSC-primary passaged 4–9 times (activated HSCs) were used in experiments. To keep consistent conditions throughout the study, oleic acids (20 μM) were added to DMEM with 10% of FBS, which did not cause LD formation in non-transduction cells but did cause LD formation in pFLRu-PLIN 5 transduced cells which may mimic LD formation in quiescent HSCs.

2.3 | Construction of PLIN 5 expressing plasmids

To construct PLIN 5 expressing plasmids, the following oligonucleotides (NCBI Reference Sequence: NM_025874.3) were used

as primers for PCR products: forward, 5′-TTG CGA GAA TTC ACC ATG GAC CAG AGA GGT GAA GAC A-3′ and reverse, 5′-GT GGC GAC CGG TCA GAA GTC CAG CTC TGG CAT CAT TG −3′. All of the PCR products contained an Eco RI restriction site at the 5′-end and an Age I at the 3′-end. The resulting PCR product (1392 bp) was digested with Eco RI and Age I and cloned into pFLRu-Vector to generate PLIN 5 expressing constructs according to Feng and Fraley's work.[25,26] Additional primer sequences are shown in Table S1.

2.4 | Measurement of TG and GSH levels

To measure the accumulation of lipids in HSC and mice livers, the content of TG was measured with commercial assay kits (Solarbio, Beijing, China). To examine the antioxidant capacity of the mouse liver, GSH levels were measured using a commercial kit (Beyotime, Nanjing, China).

2.5 | Caspase 3 activity assay

The fluorometric EnzChek® Caspase 3 Assay Kit (Cat. E13183, Invitrogen Inc) was used to detect the activity of Caspase-3 in cell lysates.

2.6 | ATP level measurement

ATP levels were determined using the ATP Determination Kit (Invitrogen). After 2 days in culture, cells were transduced with pFLRu-PLIN 5 and pFLRu-Vector, followed by ATP determination according to the manufacturer's instructions.

2.7 | Isolation of mitochondrial fraction from hepatic stellate cells

Freshly isolated rat hepatic stellate cells were used in the mitochondrial extraction kit (Solarbio) for mitochondrial extraction. The procedures for cell lysis and subsequent centrifugations were conducted following the manufacturer's protocols.

2.8 | Mitochondrial DNA copy number

Total DNA was extracted from rat HSCs using the DNeasy Blood and Tissue Kit (Qiagen, Hombrechtikon, Switzerland) following the manufacturer's instructions. An assay based on real-time quantitative PCR was used for both nDNA and mtDNA quantification using SYBR-Green as the fluorescent dye (Invitrogen).

2.9 | Histological examination

The liver tissue samples were fixed with 4% paraformaldehyde for >24 h, dehydrated, and embedded in paraffin wax using routine methods. Sections were cut (6 mm) and stained with Hematoxylin and Eosin (HE), Sirius red, and Masson's trichrome to evaluate steatosis, collagen fibrils, and liver fibrosis, respectively.

2.10 | UPLC-MS/MS analysis

Untargeted metabolomics analysis was performed on Thermo Scientific Dionex Ultimate 3000 UPLC system combined with a Q-Exactive mass spectrometer (Thermo Fisher Scientific, USA). We used ACQUITY BEH C8 (2.1 × 100 mm, 1.7 μm) for positive model detection and ACQUITY HSS T3 (2.1 × 100 mm, 1.8 μm) for negative model detection. The mass spectrometry equipped with an electrospray ionization (ESI) source was operated in both positive and negative resolution modes to obtain more differential metabolites.

2.11 | Statistical analysis

Results were expressed as means ± SD. Multi-group comparisons were performed by one-way ANOVA with Tukey's post hoc test, and the comparisons between two groups were performed by Student's t test (IBM SPSS Statistics 24). The data obtained from metabolomic profiling of mice livers were imported into SIMCA-P software (version 14.1) for multivariate statistical analysis. Data with a P value less than 0.05 were considered statistically significant.

3 | RESULTS

3.1 | Perilipin alterations take place in liver *in vitro*

Firstly, we analyzed the mRNA expression of PLIN 5 in fatty and normal livers of rats and mice and in day 1 HSCs (Quiescent HSCs) and day 7 HSCs (7-days cultured HSCs), activated primary HSCs (passaged 4–9 times), GRX cells (murine hepatic stellate cell line), and T6 (rat hepatic stellate cell line) cells. As shown in Figure 1A,B, the mRNA expression of PLIN 5 mRNA was significantly higher in visceral fats and subsequently decreased in normal livers, quiescent HSCs, and D7-HSCs, and were almost undetectable in activated primary HSCs, GRX, and T6 cells. Furthermore, we examined the expression of PLIN 5 in D1-HSCs and D7-HSCs by real-time PCR (Figure 1C) and fluorescent immunostaining (Figure S1). PLIN 5 decreased significantly in D7-HSCs compared to D1-HSCs.

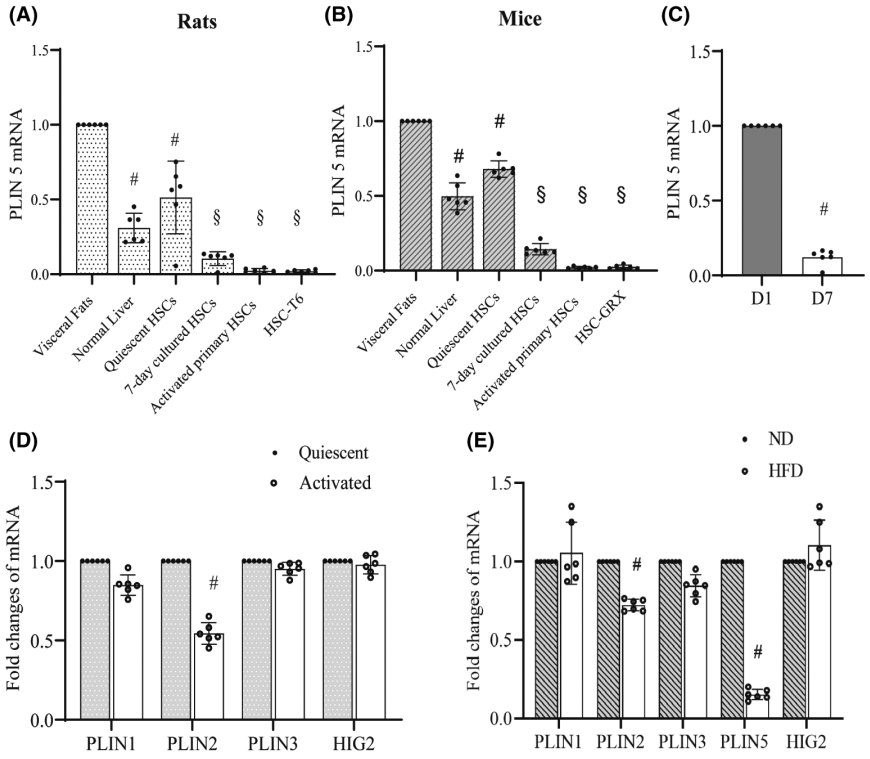

FIGURE 1 PLIN 5 quickly decreased in the process of HSC activation. (A,B), mRNA levels of PLIN 5 in different tissues or HSC populations from rats and mice were analyzed by real-time PCR. $^{\#}p<0.05$ vs fat tissues, $^{\S}p<0.05$ vs quiescent HSCs. (C), Real-time PCR analysis shows PLIN 5 mRNA levels in 1-day cultured and 7-day cultured HSCs from rats. $^{\#}p<0.05$, compared to 1-day cultured HSCs. (D), Real-time PCR analysis shows mRNA levels of other perilipin members. (E), Real-time PCR analysis shows mRNA levels of different perilipin members in HSCs from HFD-fed mice and ND mice. $^{\#}p<0.05$, compared to Chow mice HSCs. $n=6$.

Next, we studied the expression of other lipid droplet-related proteins, such as perilipin 1 (PLIN 1), PLIN 2 (ADRP), PLIN 3 (TIP47) and HIG2,[27] in quiescent vs activated HSCs (Figure 1D). PLIN 2 decreased by about 50% in mouse activated HSCs vs quiescent HSCs, and no difference was found among PLIN 1, PLIN 3, and HIG2. We also analyzed the mRNA levels of the lipid droplet-related proteins in HSCs from mice fed ND vs HFD. Both PLIN 5 (90%) and PLIN 2 (about 40%) were dramatically decreased in HSCs obtained from mice fed the HFD (Figure S1). Thus, we focused on the role of PLIN 5 in activated HSCs. Taken together, PLIN 5 showed a negative correlation with activated HSC.

3.2 | Exogenous PLIN 5 plays a role in anti-proliferation in activated HSCs

To further investigate the role of PLIN 5 in HFD-induced liver fibrosis, we selected the main effector cells of liver fibrosis (activated HSCs) as an in-vitro cell model. As we mentioned above (Figure 1), PLIN 5 is dramatically reduced during HSC activation. Therefore, we ectopically overexpressed PLIN 5 (5×10^5 TU/mL) in the primary activated HSCs (rHSC-primary) using the lentiviral system (Figure S2). Further, we studied the role of PLIN 5 in cell growth and proliferation. Interestingly, the proliferation of rHSC-primary was significantly affected upon overexpressing PLIN 5 using 20 μM OA+ pFLRu-PLIN 5, instead of 100 μM OA alone (Figure 2B), showing that the absence of PLIN 5 in activated HSCs favors the proliferation of HSCs.

Moreover, the western blotting analysis showed that ectopic overexpression of PLIN 5 suppressed the production of α-SMA, collagen (Figure 2C) and Cyclin D1, and upregulated p21 (Figure 2D), and activated HSCs cell were arrested at G1/G0 phase (Figure 2D).

Furthermore, overexpression of PLIN 5 in HSCs significantly promoted lipid droplet formation compared to the cells with aberrant expression of the PLIN 5 (Figure S3A). However, lipid droplet formation also showed up in untransduced cells incubated in DMEM containing 100 μM OA, suggesting that PLIN 5 facilitated lipid droplet formation. TG assay indicated that both 20 μM OA+ pFLRu-PLIN 5 and 100 μM OA greatly increased the levels of TG in rHSC-primary (Figure S3B).

3.3 | PLIN 5 induces apoptosis in activated HSCs that is eliminated by Z-VAD-FMK

Activation of caspase-associated proteins, especially caspase-3, is essential for executing Type I programmed cell death via various apoptotic stimuli.[28] To understand how PLIN 5 mediates proliferation arrest in activated HSCs, we determined the rate of apoptosis in PLIN 5 overexpression and PLIN 5−/− cells. rHSC-primary were transduced with lentiviral pFLRu-PLIN 5 for 48 h, which activated caspase-3 from 12 h onwards and maintained the highest levels from 18 to 48 h (Figure 3A). Next, rHSC-primary were transduced with lentiviral pFLRu-PLIN 5 and we examined the protein expression of Bcl-2 and Bax, PARP, caspase-3, and caspase-9 (Figure 3B–D), the activation of caspase cascades was observed in activated HSCs with ectopic expression of PLIN 5.

Additionally, we sought to investigate whether the blockade of caspase cascades with the pan-caspase inhibitor Z-VAD-FMK would prevent PLIN 5-induced cell cycle arrest. rHSC-primary cells

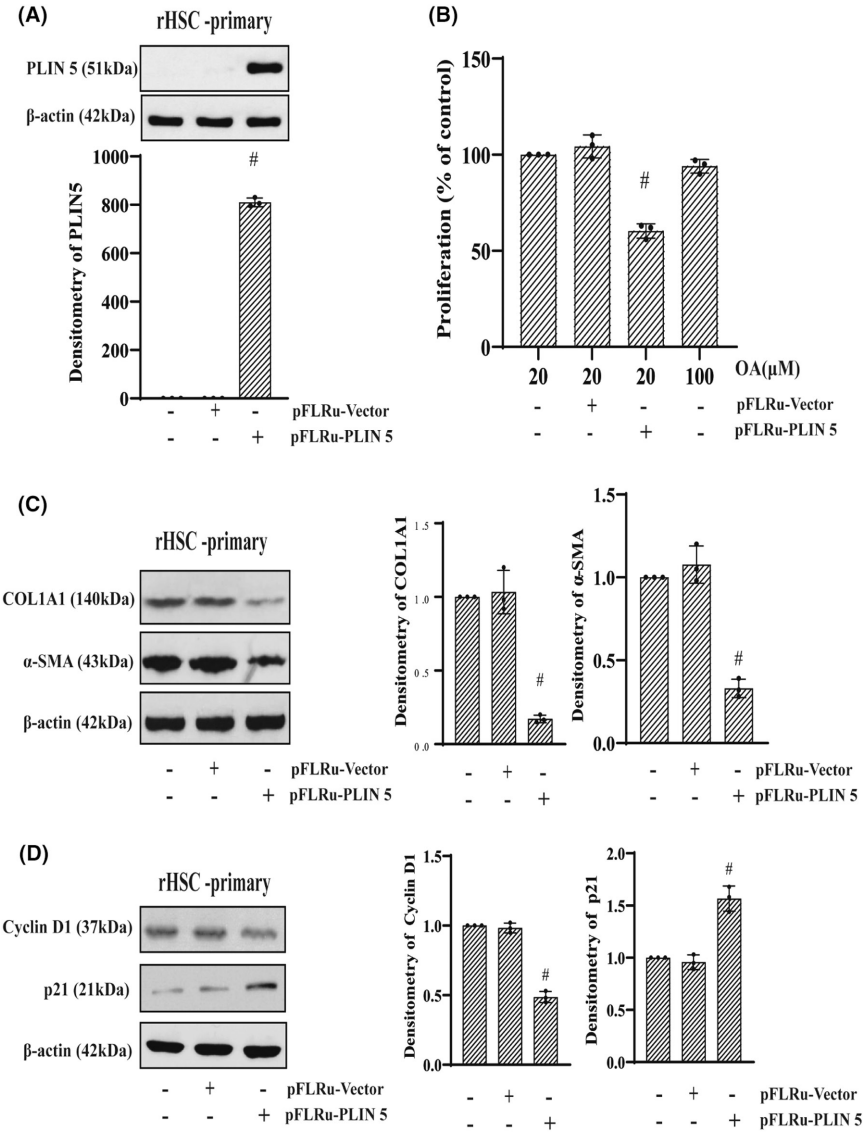

FIGURE 2 Exogenous expression of PLIN 5 inhibits proliferation in activated HSCs. (A), Western blotting (upper panel) and real-time PCR (lower panel) show the efficacy of lentiviral transduction in primary HSCs. β-Actin is used as a loading control. (B), The proliferation of rat primary HSCs transduced with pFLRu-PLIN 5 was determined by MTS. (C), Fibrotic markers of rat primary HSCs transduced with pFLRu-PLIN 5 were determined by western blotting analysis. The bar charts on the right show the densitometry of COL1A1 and α-SMA. (D), Western blot of Cyclin D1 and p21, cell cycle-associated proteins, in rat primary HSCs transduced with pFLRu-PLIN 5. The bar charts on the right show the densitometry of Cyclin D1 and p21. $^{\#}p < 0.05$ comparing with untreated control, $n = 3$. β-Actin was used as a loading control.

containing pFLRu-PLIN 5 were pretreated with the pan-caspase inhibitor Z-VAD-FMK (50 μM) for 1 h, which completely prevented PLIN 5-induced apoptosis and proliferation arrest (Figure 3E–I) Taken together, our results demonstrate that exogenous expression of PLIN 5 induces apoptosis in activated HSCs via the activating caspase cascades.

3.4 | PLIN 5 mediated anti-proliferation and apoptosis in HSC by activating AMPK

We sought to evaluate whether PLIN 5 regulates AMPK in HSCs, which is known to induce proliferation arrest and apoptosis. To activate AMPK, rHSC-primary cells were treated with AICAR (1.0 mM, an AMPK activator), which decreases ATP levels by inhibiting mitochondrial respiratory chain complex 1,[29] and which was used as a positive control. Exposure to AICAR decreased the proliferation of the rHSC-primary cells (Figure 4A) and increased caspase-3 activity (Figure 4B). In addition, the rHSC-primary cells were transduced with lentiviral pFLRu-PLIN 5. Phosphorylation of AMPK (Thr172) was assessed by western blot, showing that expression of PLIN 5 elicited AMPK activity (Figure 4C). These results suggest that PLIN 5 overexpression can mimic the AMPK activation induced by AICAR.

To confirm the role of AMPK in mediating PLIN 5-induced proliferation arrest, rHSC-primary cells were treated with compound C, a well-established pharmacological inhibitor of AMPK activity, for 1 hour. As shown in Figure 4D–J, compound C reversed the PLIN 5-induced cell cycle arrest and apoptosis. Taken together, these data demonstrate that activation of AMPK is involved in PLIN 5-mediated proliferation arrest and apoptosis in activated HSCs.

3.5 | PLIN 5-induced mitochondrial dysfunction contributes to AMPK activation, and hence to anti-proliferation and apoptosis induction in activated HSCs

Firstly, we evaluated the role of PLIN 5 in the regulation of PGC-1α expression in HSCs, simply by transducing rHSC-primary cells with lentiviral pFLRu-PLIN 5. The results showed that overexpression

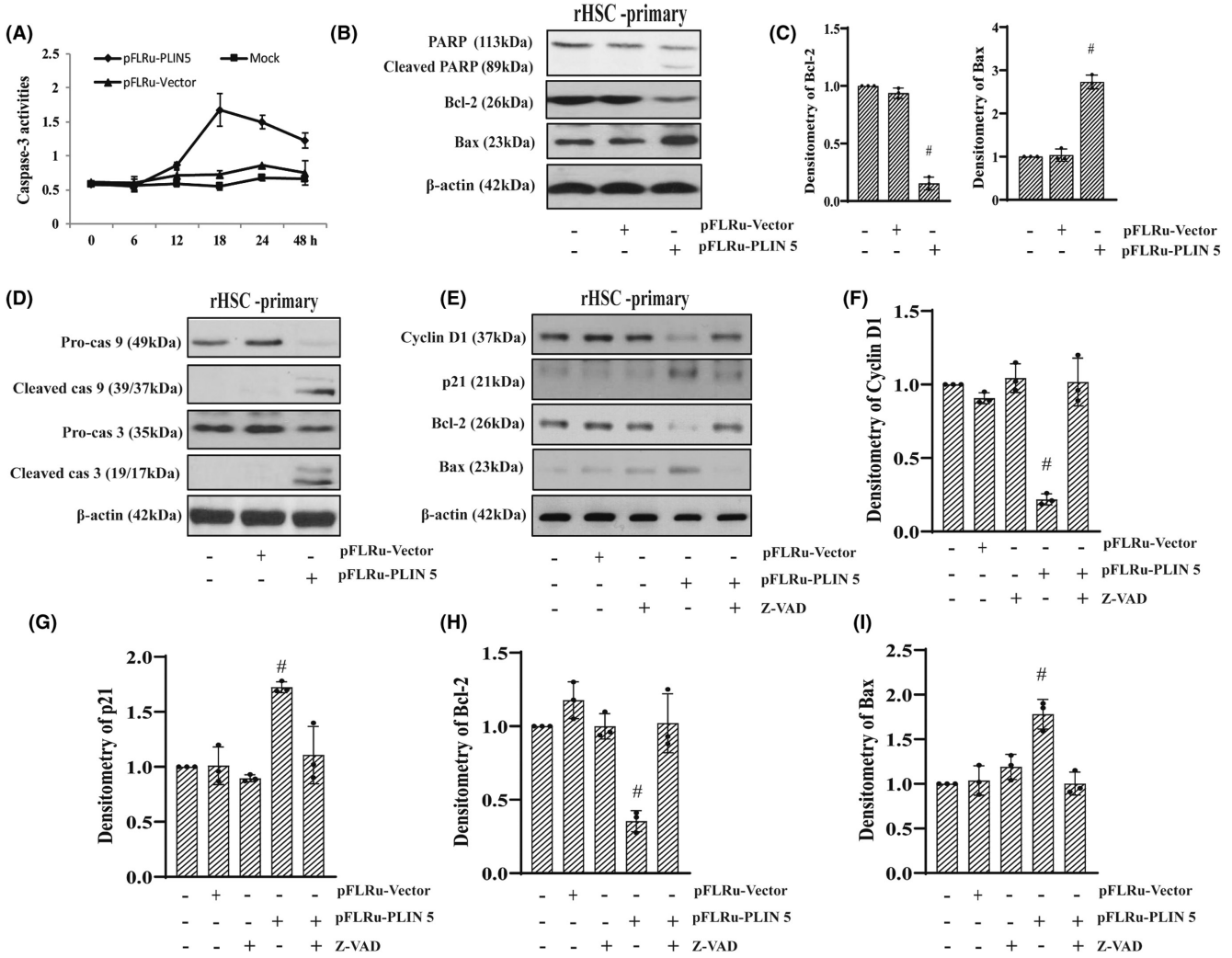

FIGURE 3 PLIN 5 mediated apoptosis in HSCs. (A), Caspase-3 activity assay in activated rat primary HSCs with pFLRu-PLIN 5. (B), Western blotting analysis shows an expression of pro-apoptotic genes (PARP, Bcl-2, and Bax) in rat primary HSCs after transduction with pFLRu-PLIN 5. (C), The bar charts show the densitometry of Bcl-2 and Bax, respectively. (D), Western blotting analysis shows an expression of caspase cascades (caspase-3, -9) in rat primary HSCs after transduction with pFLRu-PLIN 5. (E), Western blotting analysis shows an expression of Bcl-2 and Bax and Cyclin D1 and p21 in rat primary HSCs pretreated with the pan-caspase inhibitor Z-VAD-FMK (50 μM) for 1 h and followed by transduction of pFLRu-PLIN 5. (F–I), Bar charts show the densitometry of Cyclin D1, p21, Bcl-2, and Bax, respectively. Data are expressed as means ± SD. $^{\#}p < 0.05$ vs. untreated cells. Representatives are from three independent experiments.

of PLIN 5 decreased the level of PGC-1α mRNA in activated HSCs *in vitro* (Figure 5A). Given that PLIN 5 disturbed the mitochondrial function, we subsequently examined the levels of ATP in activated HSCs transduced with PLIN 5. Our results showed that overexpression of PLIN 5 led to a reduction in ATP levels in rHSC-primary cells (Figure 5B). When PLIN 5 was overexpressed in HSC-primary cells, cell proliferation decreased compared with the normal control group (Figure 5C). The expression of caspase 3 in the PLIN 5 overexpression group was higher than that in the normal group, and apoptosis increased (Figure 5D). When we exogenously supplemented activated hepatic stellate cells with MP, a pyruvate lipid derivative, to increase the mitochondrial metabolism level, proliferation inhibition and apoptosis of activated hepatic stellate cells with lentiviral pFLRu-PLIN 5 expression were eliminated (Figure 5C–J). MP provides energy for the tricarboxylic acid cycle to produce NADH. Therefore, we hypothesized that the reversal of activation of hepatic stellate cells by PLIN 5 is mainly closely related to the metabolic level of mitochondria.

Our previous experimental results suggested that phosphorylated AMPK (P-AMPK) is involved in the apoptosis of activated hepatic stellate cells induced by high expression of PLIN 5 (Figure 4). To further explore the role of PLIN 5 in apoptosis, we added the caspase inhibitor Z-VAD-FMK to activated hepatic stellate cells with high PLIN 5 expression. The results showed that Z-VAD-FMK abrogated the apoptosis induced by PLIN 5 (Figure 5L). Western blotting also indicated that Z-VAD-FMK inhibited the apoptosis of activated hepatic stellate cells with high PLIN 5 expression independently of P-AMPK (Figure 5K). However, when we exogenously added the mitochondrial agonist MP, MP not only reversed the PLIN 5 overexpression-induced P-AMPK overexpression profile

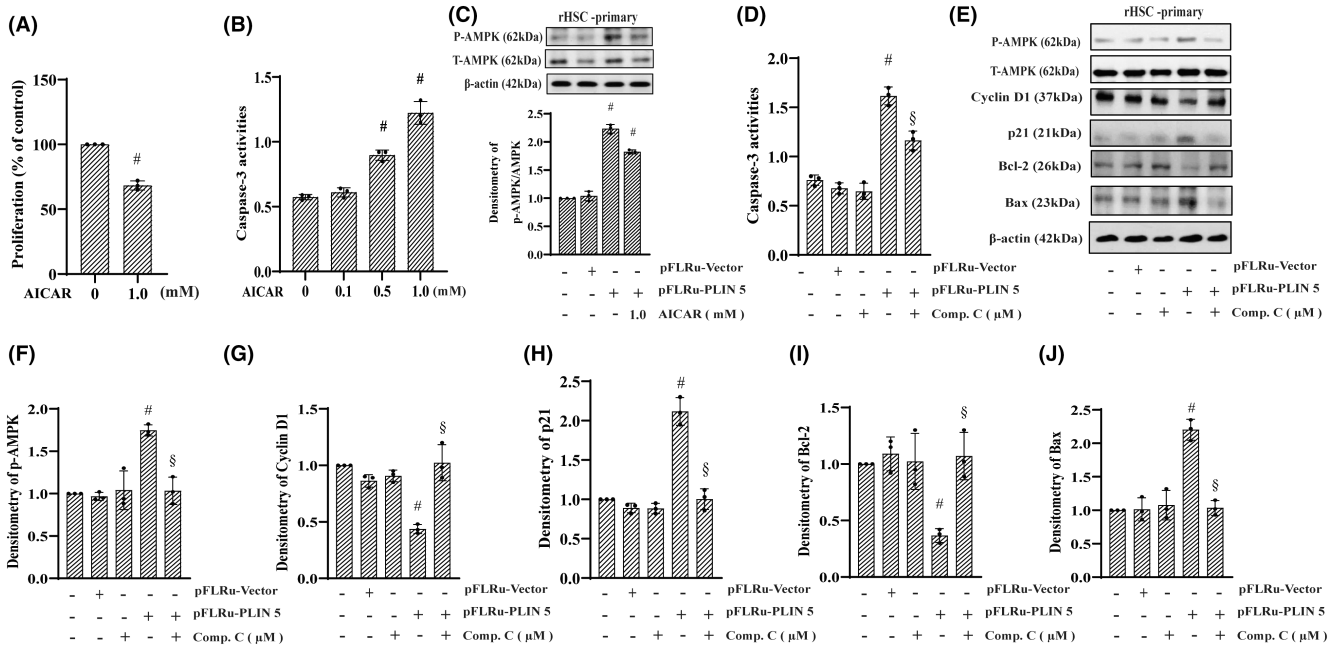

FIGURE 4 Activation of AMPK is required for PLIN5-mediated anti-proliferation and apoptosis in HSCs. (A), The proliferation of rat primary HSCs treated with AICAR at 1.0 mM for 24 h was determined by MTS. (B), Caspase-3 activity assay in rat primary HSCs treated with AICAR at different dosages for 24 h. (C), Rat primary HSCs were transduced with pFLRu-PLIN 5 or AICAR (1.0 mM) for 24 h. Phosphorylation of AMPK (Thr172) and total AMPK were determined by western blotting analysis. The lower panel shows the densitometry of phos-AMPK/t-AMPK. (D), Rat primary HSCs were pretreated with compound C (10 μM), a specific inhibitor of AMPK, for 1 h, followed by transduction of pFLRu-PLIN 5 in a medium with compound C. Caspase-3 activity was determined as described in Methods. (E), Phosphorylation of AMPK, total AMPK, Bcl-2, Bax, and Cyclin D1, p21 were determined by western blotting analysis. (F–J), Bar charts show the densitometry of p-AMPK/t-AMPK, Cyclin D1, p21, Bcl-2, and Bax, respectively. The results are representative of three independent experiments. Data are expressed as means ± SD. $^{\#}p < 0.05$ vs untransduced cells, and $^{\S}p < 0.05$ vs pFLRu-PLIN 5 group, $n = 3$.

(Figure 5K), but also abrogated PLIN 5-induced apoptosis (Figure 5L). This suggests that the addition of MP reduced the apoptosis of PLIN 5 overexpressing hepatic stellate cells. These results imply that mitochondria play an important role in influencing AMPK phosphorylation levels. Mitochondria are involved in apoptosis induced by activated HSCs with PLIN 5 overexpression by regulating their own energy metabolism levels.

Finally, we evaluated the role of PLIN 5 in the biogenesis of the mitochondria. rHSC-primary cells were transduced with lentiviral pFLRu-PLIN 5. A significant reduction in the mitochondrial DNA copy number variations, citrate synthase activity (Figure S4A,B), and PGC-1α expression (Figure S4C,D) was observed after exogenous expression of PLIN 5. These data indicate that PLIN 5 suppresses mitochondrial biogenesis thus inducing proliferation arrest and apoptosis via AMPK activation in activated HSCs.

3.6 | Knockout of PLIN 5 reverses insulin resistance, steatosis, and fibrosis in HFD-induced steatohepatitis

We performed NAFLD studies using C57BL/6J mice and PLIN 5−/− mice (Figure 6A,C). We examined the blood glucose levels in mice by IPGTT and ITT. The glucose concentration in HFD mice increased significantly over time. When PLIN 5 was knocked out, the glucose homeostasis was significantly improved (Figure S5). We evaluated the protein levels of hepatic COL1A1 and αSMA, two pro-fibrotic proteins. The protein levels of COL1A1 and α-SMA were greatly increased in HFD-fed C57BL/6J mice compared to ND-fed C57BL/6J mice (Figure 6B,D,E). The antifibrotic effect of PLIN 5−/− on NAFLD was associated with reduced expression of COL1A1 I and α-SMA.

HFD fed C57BL/6J mice developed NAFLD with severe steatosis covering a 70%–95% hepatic area while PLIN 5−/− mice accumulated significantly lower fat and showed lower amounts of ballooning degeneration of hepatocytes. The size and number of lipid droplets (LD) in the liver tissues of the PLIN 5−/− HFD group were significantly reduced compared to HFD-treated C57BL/6J mice (Figure 6F,J,K). The livers of C57BL/6J mice and PLIN 5−/− mice fed with ND did not exhibit fibrosis and collagen deposition. Large vesicular hepatic steatosis, fibrosis, and collagen deposition were seen in the livers of C57BL/6J mice in the HFD group compared to ND-fed C57BL/6J mice. Fibrosis and collagen deposition was significantly reduced in the livers of HFD-fed PLIN 5−/− mice compared to C57BL/6J mice fed HFD (Figure 6G,H,L,M). In addition, HFD-fed C57BL/6J mice showed increased hepatic triacylglycerol content compared to ND-fed C57BL/6J mice. -In HFD-fed PLIN5-/- mice, the fibrosis in the liver was alleviated and the intrahepatic triacylglycerol content was reduced (Figure 6N). Moreover, PLIN 5−/− mice had significantly

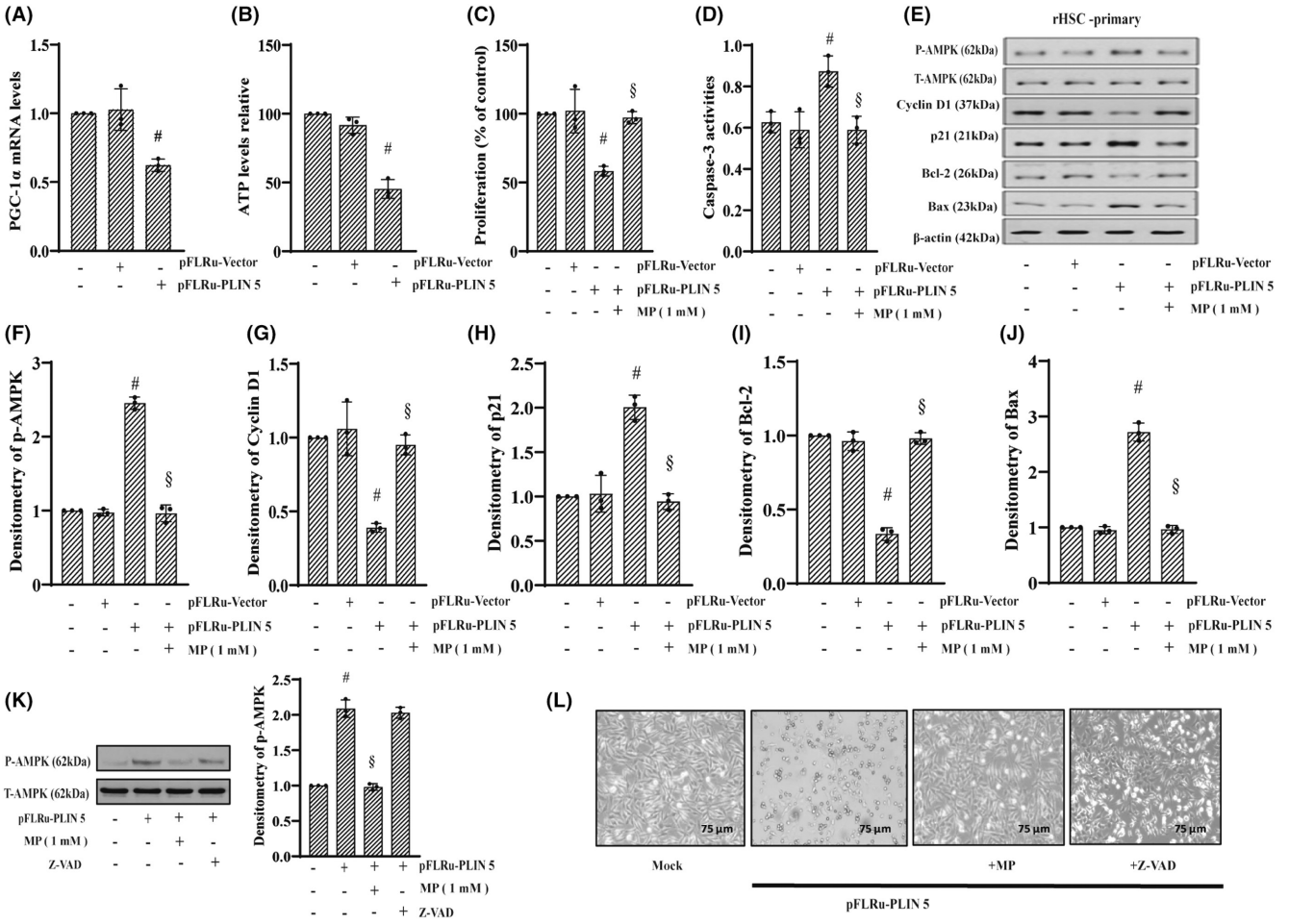

FIGURE 5 PLIN 5-induced mitochondrial dysfunction is required for apoptosis via AMPK activation in activated HSCs. (A–D), mRNA expression levels of PGC-1a (A), total ATP contents (B), cell proliferation (C), and caspase-3 activities (D) were detected in rat primary HSCs pretreated with MP (1 mM) for 2 h, followed by transduction of pFLRu-PLIN 5. (E), Western blotting analysis for expression of Cyclin D1, p21, Bcl2, and Bax in rat primary HSCs pretreated with MP (1 mM) for 2 h, followed by transduction of pFLRu-PLIN 5. (F–J), Bar charts show the densitometry of the target genes in panel E. (K), Phosphorylation of AMPK in rat primary HSCs pretreated with MP (1 mM) for 2 h or Z-VAD-FMK (50 μM) for 1 h and then transduced with pFLRu-PLIN 5, respectively. $^{\#}p < 0.05$ vs untreated cells, $^{\S}p < 0.05$ vs pFLRu-PLIN 5 group, $n = 3$. The results are representative of three independent experiments. (L), Images were captured under the inverted phase-contrast microscopy (20×) in rat primary HSCs pretreated with Z-VAD-FMK (50 μM) or supplementation of MP (1 mM) for 1 h before transduction of pFLRu-PLIN 5.

reduced uptake of fatty acids, and fatty acid synthesis was also inhibited (Figure 6I). These results indicated that PLIN 5−/− may be involved in the reversal of HFD-induced liver fibrosis.

3.7 | Metabolic profile of liver tissues in C57BL/6J and PLIN 5−/− mice fed an HFD

To investigate the metabolic dysregulation, we performed untargeted metabolomic profiling of mouse liver using the Thermo Scientific Dionex Ultimate 3000 UPLC system combined with a Q-Executive mass spectrometer. OPLS-DA score plots and permutation tests demonstrated a remarkable separation tendency among the four groups, indicating that the metabolic conditions of the C57BL/6J ND, PLIN 5−/− ND, C57BL/6J HFD, and PLIN 5−/− HFD samples were notably changed in both positive and negative ion modes (Figure 7A,B). A total of 47 significant differential metabolites were identified by matching with the corresponding spectrograms of METLIN, HMDB, and other public databases (Figure 7C). Metabolite set enrichment analysis of all measured metabolites in HFD-fed C57BL/6J and PLIN 5−/− mice identified glutamate and glutathione metabolism as one of the mainly impacted pathways (Figure 7D). To confirm these results, GSH was measured with the Micro Reduced Glutathione (GSH) Assay Kit, which showed a significant decrease in the concentration of GSH in the C57BL/6J HFD group compared to the PLIN 5−/− HFD group (Figure 7E). Next, gene expressions of Gclc and Gclm were measured by RT-PCR. As expected, the amounts of Gclc and Gclm were significantly reduced in the C57BL/6J HFD group compared with PLIN 5−/− mice HFD group (Figure 7F).

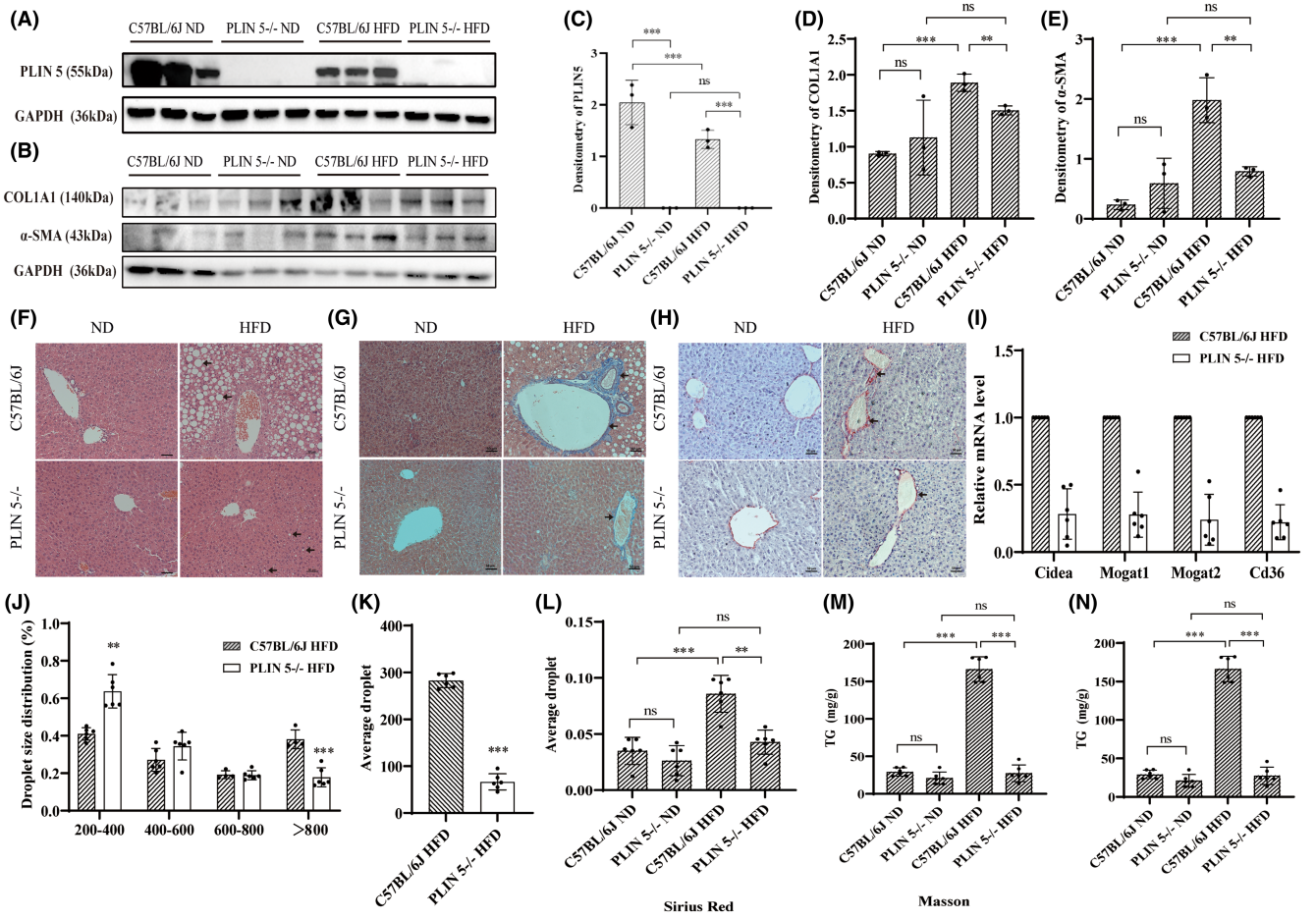

FIGURE 6 PLIN 5−/− reverses liver injury, steatosis, and fibrosis in HFD-induced steatohepatitis. (A–E), The protein levels of PLIN 5 (A and B) and the results of COL1A1 and α-SMA protein expression (C, D, and E) in each group of mice. (F–H), H&E staining (F), Masson' trichrome (G) and Sirius Red staining (H) of the liver sections of different groups. (I), mRNA expression levels of fatty acid synthesis-related genes were analyzed by PCR. (J and K), The average number of lipid droplets (J) and average droplet size (K) in C57BL/6J and PLIN 5−/− mice fed a HFD. (L and M), Blind calculation of fibrotic foci per field in Masson and Sirius Red staining slides. Data were generated from 3 random fields per slide, 6 mice/genotype. (N), Triglyceride (TG) content in the liver of four groups. Results are means ± SD ($n = 6$). $^{*}p < 0.05$; $^{**}p < 0.01$, $^{***}p < 0.001$.

3.8 | PLIN 5 deletion suppresses HFD-induced mitochondrial dysfunction and apoptosis through AMPK/PGC1α

To explore the underlying mechanisms of PLIN 5 in NAFLD, we assessed the expression of mitochondrial biosynthesis, cell proliferation, and inflammation-related genes by RT-PCR, which showed that PLIN 5−/− mice with NAFLD had significantly decreased mitochondrial biosynthesis-related genes (PGC-1α, mtTFA, UCP1) and oxidative stress-related gene (Gstm3. Gpx3, Cbr3) mRNA levels were significantly decreased (Figure 8A,B). Compared to C57BL/6J mice, PLIN 5−/− mice fed the HFD showed reduced levels of proliferation-related gene mRNA (Figure 8C). Meanwhile, the expression of pro-inflammatory cytokines (Cxcl4, TNF α, Ccr2, Ly6c) was increased in the C57BL/6J HFD group (Figure 8D).

Results from the study of AMPK activation in the liver showed significant inhibition of AMPK activity in the liver tissues of HFD-fed C57BL/6J mice, while p-AMPKα was significantly upregulated in the PLIN 5−/− HFD group (Figure 8F). To further study the beneficial mechanism(s) of PLIN 5−/− in HFD, we also measured the expression of Bcl-2, Bax, and caspase 3 data showed downregulation of Bcl-2, upregulation of Bax and caspase 3 in HFD fed PLIN 5−/− mice (Figure 8G,H). These results demonstrate that PLIN 5−/− protected liver from HFD-induced hepatic apoptosis.

4 | DISCUSSION

Activation of hepatic stellate cells (HSCs) is a major contributor to liver fibrosis.[30] In NAFLD induced by a HFD, HSCs are activated in response to abnormal lipid accumulation and inflammation within the liver.[31] As a result, HSCs lose their ability to store lipid droplets, undergo trans-differentiation into myofibroblast-like cells, and increase the expression of α-SMA and collagen, eventually leading to liver fibrosis.[32] In this project, we observed that the expression of PLIN 5, a protein associated with lipid droplets,[33] decreased with

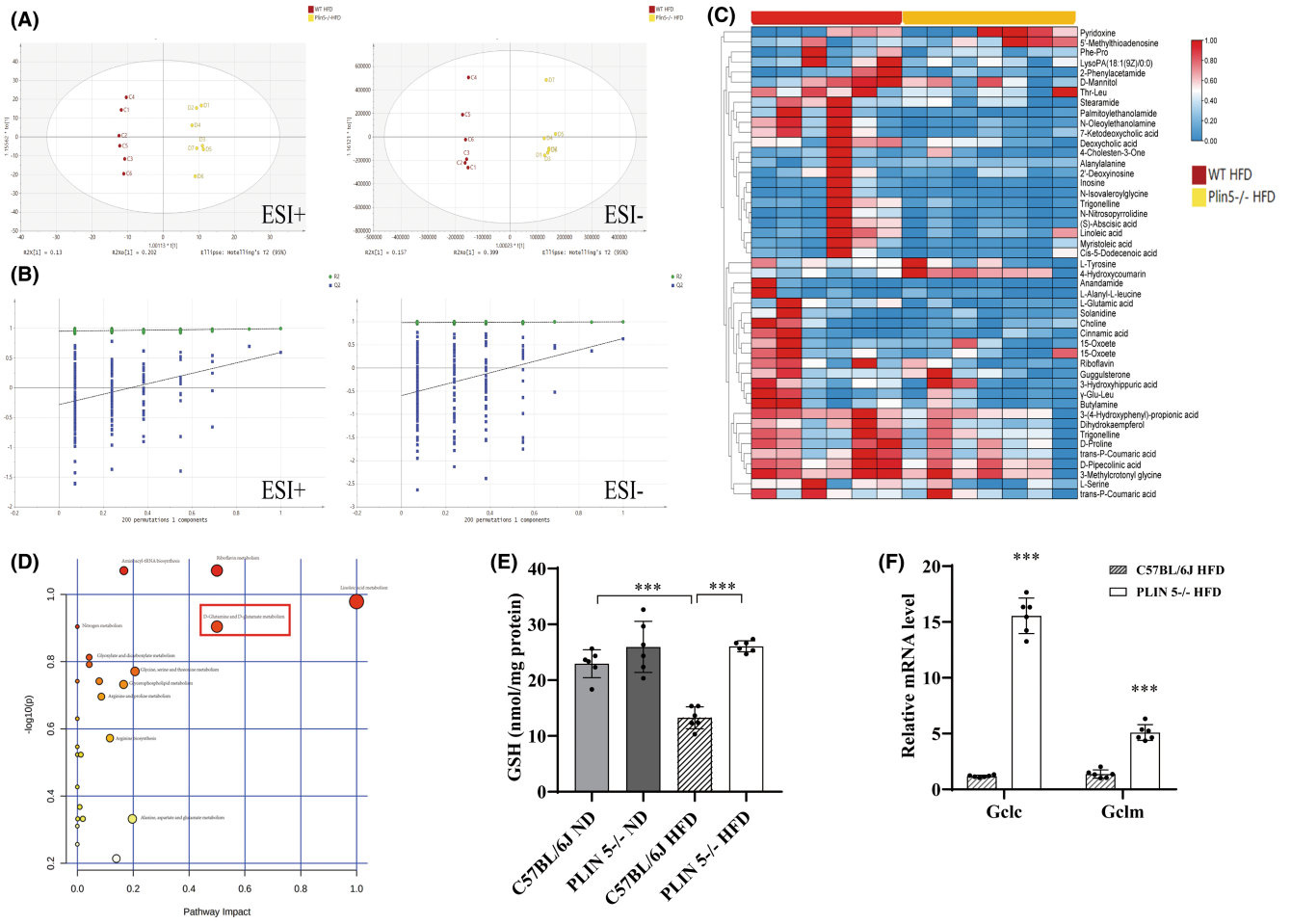

FIGURE 7 Metabolic profile of liver tissues in C57BL/6J and PLIN 5−/− mice fed an HFD. (A), The score chart of OPLS-DA in liver tissue samples in ESI+ and ESI−, respectively. (Red dots: C57BL/6J HFD, yellow dots: PLIN 5−/−HFD). (B), The permutation test analysis by OPLS-DA in liver samples was evaluated in positive ion mode (ESI+) and negative ion mode (ESI−), respectively. (C), The heatmap of the 47 differential metabolites with hierarchically clustering analysis (VIP >1 and $p < 0.05$). Color change from blue to red indicates that changes in metabolite concentrations from low to high. (D) Differential metabolite association analysis. (D), The impact on pathways in liver tissue among C57BL/6J and PLIN 5−/− mice fed a HFD. (The abscissa 'pathway impact' represents the impact value of the pathway, and the ordinate −log (p) represents the result of statistical analysis.) (E), GSH levels in liver tissue of the four groups. (F), Quantitative PCR (qPCR) of gene expression for Gclc and Gclm. Gene expression is normalized to GAPDH. Data were expressed as means ± SD ($n = 6$). ***$p < 0.001$.

the loss of lipid droplets in the cytoplasm of activated HSCs. This suggests that PLIN 5 expression is negatively correlated with HSC activation. To further investigate this relationship, we used activated rHSC-primary cells as an in vitro model and employed a lentiviral vector to stably overexpress PLIN 5 in these cells. By doing so, we were able to explore the mechanisms by which PLIN 5 activates HSCs and its potential influence on the development and progression of non-alcoholic fatty liver disease.

AMPK is a key regulator of energy metabolism in cells, which is activated in response to increased AMP/ATP ratios, calcium levels, and LKB1 signaling.[34] Previous studies have demonstrated that activation of AMPK can inhibit the proliferation and induce apoptosis of activated HSCs, which play a critical role in liver fibrosis.[35] Therefore, we focused on studying the regulatory effect of PLIN 5 on HSCs through the AMPK signaling pathway. We were able to confirm that PLIN 5 overexpression in activated HSCs leads to increased AMPK phosphorylation, as well as inhibition of HSC proliferation and promotion of cell apoptosis. To further validate these findings, we conducted a control experiment using the AMPK inhibitor compound C, which confirmed that activation of AMPK is necessary for PLIN 5 to induce cell death.

Accumulating evidence indicates that mitochondrial dysfunction plays a key role in activated HSCs, although the mechanisms underlying this dysfunction are still unclear.[36–38] The main function of mitochondria is to carry out oxidative phosphorylation (OXPHOS) to synthesize ATP, and mitochondria are the site of the final oxidation of sugars, fats and amino acids to release energy.[39] Therefore, we first analyzed mitochondrial function by changing PLIN 5 expression in in vitro-cultured rHSC-primary cells. We found that PLIN 5 overexpression in activated HSCs resulted in a decrease in ATP levels within the mitochondria, inhibition of cell proliferation, and a significant increase in cell apoptosis. To further explore

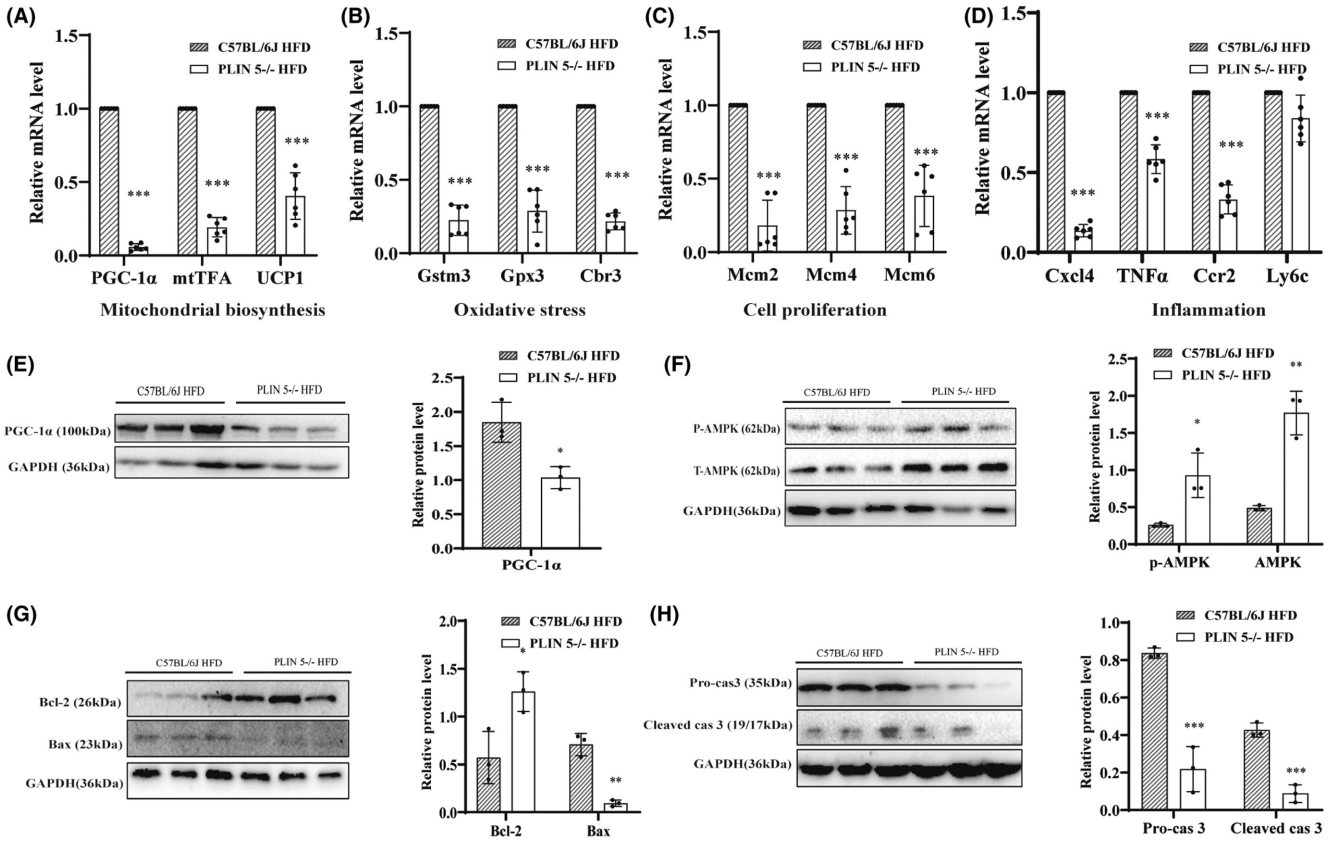

FIGURE 8 Effect of PLIN 5 −/− on HFD-induced liver oxidative stress, inflammation, and extracellular matrix organization. (A), mRNA expression levels of Mitochondrial biogenesis-related genes PGC-1α, mtTFA, UCP1). (B–D), Oxidative stress genes (Gstm3, Gpx3, Cbr3) (B), cell proliferation-related genes (Mcm2, Mcm4, Mcm6) (C), and inflammatory response-related genes (Cxcl14, Cxcl2, Ly6c) (D). (E–H), Representative western blotting and the densitometry analysis of PGC-1α (E), p-AMPK and AMPK (F), Bcl-2 and Bax (G), Pro-cas 3, and cleaved caspase-3 (H) in the liver tissue in two HFD groups. Data were expressed as means ± SD ($n = 6$). *$p < 0.05$; **$p < 0.01$, ***$p < 0.001$.

this mechanism, we exogenously supplemented MP to provide energy for the mitochondrial tricarboxylic acid cycle. MP eliminated the effect of PLIN 5 in activated HSCs. These results suggest that PLIN 5-induced apoptosis of activated HSC cells may be related to the energy metabolic level of the mitochondria. In addition, in this experiment, we found that PLIN 5 overexpression in activated HSCs leads to reduced mtDNA copy number[40] and citrate synthase activity (the first step in the tricarboxylic acid cycle),[41] as well as decreased abundance of PGC-1α, compared to untreated HSCs. These data suggest that the mitochondria play a crucial role in the process of inhibiting cell proliferation and enhancing cell apoptosis through PLIN 5. Studies have also shown that the mitochondria play a significant role in the development and progression of NAFLD, involving regulation of ATP metabolism and mitochondrial dysfunction. However, the underlying mechanisms behind these processes remain to be further explored.

To investigate the mechanism of PLIN 5 in the development of NAFLD, we conducted in vivo experiments using a mouse model. UPLC/MS–MS technology was utilized to analyze the molecular mechanisms of the effect of PLIN 5−/− on HFD-induced fatty liver. The results show that the relevant metabolic pathway is mainly enriched in the glutathione metabolic pathway. Glutathione is an efficient antioxidant present in mitochondria, consisting of superoxide dismutase and glutathione.[42] Glutamate-cysteine ligase (GCL) is the rate-limiting enzyme of glutathione biosynthesis, consisting of GCLC (catalytic subunit) and GCLM (regulatory subunit).[43] An increase of GCL accelerates an increase in the rate of GSH biosynthesis in the body, ultimately leading to an increase in GSH content.[44] This is consistent with our experimental results. Our research has revealed that PLIN 5−/− can inhibit the decline of GSH in the liver. Other researchers have found that a decrease in GSH content is a potential early activation signal for apoptosis, and subsequent generation of oxygen free radicals leads to apoptosis.[45] This is supported by the observation that PLIN 5 knockout mice fed a HFD had fewer apoptosis-related proteins in their liver proteins compared to mice on a HFD without the PLIN 5 knockout. These findings suggest that PLIN 5−/− may have a protective effect against the development of NAFLD by combating oxidative stress.

PGC-1α, a transcriptional cofactor, activates the biogenesis of mitochondria,[46] while activated AMPK can decrease hepatic triglycerides and increase fatty acid oxidation in the mitochondria.[47] Our findings indicate that PGC-1α levels and AMPK activity are altered in the livers of mice with NAFLD. This may be due to the increased oxidative stress and inflammatory

response that occurs during the development of NAFLD, leading to increased mitochondrial synthesis metabolism. Our results also show that, the phosphorylation of AMPK is reduced in HFD-fed PLIN 5−/− mice, compared to C57BL/6J mice fed a HFD. The results of the in vivo experiments appear to be somewhat contradictory to the findings of previous in vitro experiments involving the culture of rHSC-primary cells. PLIN 5 knockout significantly delayed liver steatosis and the development of NAFLD in mice. Based on the results of experiments conducted in an in vitro model of activated HSCs, we initially hypothesized that PLIN 5−/− mice would be more sensitive to liver damage caused by a HFD and more prone to liver fibrosis. However, the experimental results are contrary to our conjecture. We obtained conflicting results.

In vivo experiments showed that PLIN 5−/− mice had reduced fibrosis and significantly improved insulin resistance. PLIN 5 knockout significantly delayed liver steatosis and the development of NAFLD in mice. These results may be due to the fact that parenchymal cells, which make up about 70% of total hepatocytes in the liver, are the dominant cell type in the liver.[48] HSCs only account for 8%–13% of the total hepatocytes.[49] We knocked out the PLIN 5 gene in all tissue cells in mice, not just in HSCs, which is a limitation of our experiment. This paradox is also related to the fact that hepatocytes and HSCs perform different physiological functions in vivo, and again emphasizes the importance of in vivo models in understanding complex systems. In future studies, we will use mice with tissue-specific deletions of PLIN 5 targeting hepatocytes or HSCs, which may resolve these issues.

AUTHOR CONTRIBUTIONS

Experiments were performed by Youcai Tang, Xuecui Yin, Lin Dong, Xiaohan Wang with the help of Yuying Ma, Zhenzhen Qin, and Yang Mi. Experiments were designed by Youcai Tang, Ya Li, and Xiaofei Ke managed animals. Xuecui Yin and Qingde Wang managed HFD-mice. Youcai Tang, Xuecui Yin, Lin Dong, Xiaohan Wang, and Quanjun Lyu analyzed the data. Youcai Tang wrote the paper, with assistance from Pengyuan Zheng and Xia Xu in editing and revisions. Youcai Tang, Pengyuan Zheng, and Xia Xu supervised the work.

ACKNOWLEDGMENTS

The authors gratefully acknowledge support for this work from funding bodies. Furthermore, we thank Dr. Ihtisham Bukhari (Gastroenterology, The Fifth Affiliated Hospital, Zhengzhou University, Zhengzhou, Henan, China) for his linguistic assistance.

CONFLICT OF INTEREST STATEMENT

The authors declare no conflict of interest.

ORCID

Xuecui Yin https://orcid.org/0000-0003-0355-9435
Lin Dong https://orcid.org/0000-0001-8769-5447

REFERENCES

1. Friedman SL, Neuschwander-Tetri BA, Rinella M, Sanyal AJ. Mechanisms of NAFLD development and therapeutic strategies. *Nat Med*. 2018;24(7):908-922. doi:10.1038/s41591-018-0104-9
2. de Oliveira S, Houseright RA, Graves AL, et al. Metformin modulates innate immune-mediated inflammation and early progression of NAFLD-associated hepatocellular carcinoma in zebrafish. *J Hepatol*. 2019;70(4):710-721. doi:10.1016/j.jhep.2018.11.034
3. Higashi T, Friedman SL, Hoshida Y. Hepatic stellate cells as key target in liver fibrosis. *Adv Drug Deliv Rev*. 2017;121:27-42. doi:10.1016/j.addr.2017.05.007
4. Tsuchida T, Friedman SL. Mechanisms of hepatic stellate cell activation. *Nat Rev Gastroenterol Hepatol*. 2017;14(7):397-411. doi:10.1038/nrgastro.2017.38
5. Roehlen N, Crouchet E, Baumert TF. Liver fibrosis: mechanistic concepts and therapeutic perspectives. *Cell*. 2020;9(4):875. doi:10.3390/cells9040875
6. Najt CP, Khan SA, Heden TD, et al. Lipid droplet-derived monounsaturated fatty acids traffic via PLIN5 to allosterically activate SIRT1. *Mol Cell*. 2020;77(4):810-824.e8. doi:10.1016/j.molcel.2019.12.003
7. Sztalryd C, Brasaemle DL. The perilipin family of lipid droplet proteins: gatekeepers of intracellular lipolysis. *Biochim Biophys Acta Mol Cell Biol Lipids*. 2017;1862(10 Pt B):1221-1232. doi:10.1016/j.bbalip.2017.07.009
8. Keenan SN, Meex RC, Lo JCY, et al. Perilipin 5 deletion in hepatocytes remodels lipid metabolism and causes hepatic insulin resistance in mice. *Diabetes*. 2019;68(3):543-555. doi:10.2337/db18-0670
9. Gemmink A, Daemen S, Kuijpers HJH, et al. Super-resolution microscopy localizes perilipin 5 at lipid droplet-mitochondria interaction sites and at lipid droplets juxtaposing to perilipin 2. *Biochim Biophys Acta Mol Cell Biol Lipids*. 2018;1863(11):1423-1432. doi:10.1016/j.bbalip.2018.08.016
10. Li H, Yu XH, Ou X, Ouyang XP, Tang CK. Hepatic cholesterol transport and its role in non-alcoholic fatty liver disease and atherosclerosis. *Prog Lipid Res*. 2021;83:101109. doi:10.1016/j.plipres.2021.101109
11. Zhang W, Xu L, Zhu L, Liu Y, Yang S, Zhao M. Lipid droplets, the central hub integrating cell metabolism and the immune system. *Front Physiol*. 2021;12:746749. doi:10.3389/fphys.2021.746749
12. Chen A, Tang Y, Davis V, et al. Liver fatty acid binding protein (L-Fabp) modulates murine stellate cell activation and diet-induced nonalcoholic fatty liver disease. *Hepatology*. 2013;57(6):2202-2212. doi:10.1002/hep.26318
13. McCommis KS, Hodges WT, Brunt EM, et al. Targeting the mitochondrial pyruvate carrier attenuates fibrosis in a mouse model of nonalcoholic steatohepatitis. *Hepatology*. 2017;65(5):1543-1556. doi:10.1002/hep.29025
14. Tang Y, Chen A. Curcumin protects hepatic stellate cells against leptin-induced activation in vitro by accumulating intracellular lipids. *Endocrinology*. 2010;151(9):4168-4177. doi:10.1210/en.2010-0191
15. Xu H, Zhao Q, Song N, et al. AdipoR1/AdipoR2 dual agonist recovers nonalcoholic steatohepatitis and related fibrosis via endoplasmic reticulum-mitochondria axis. *Nat Commun*. 2020;11(1):5807. doi:10.1038/s41467-020-19668-y
16. Montgomery MK, Mokhtar R, Bayliss J, et al. Perilipin 5 deletion unmasks an endoplasmic reticulum stress-fibroblast growth factor 21 axis in skeletal muscle. *Diabetes*. 2018;67(4):594-606. doi:10.2337/db17-0923
17. Zhang E, Cui W, Lopresti M, et al. Hepatic PLIN5 signals via SIRT1 to promote autophagy and prevent inflammation during fasting. *J Lipid Res*. 2020;61(3):338-350. doi:10.1194/jlr.RA119000336

18. Kolleritsch S, Kien B, Schoiswohl G, et al. Low cardiac lipolysis reduces mitochondrial fission and prevents lipotoxic heart dysfunction in perilipin 5 mutant mice. *Cardiovasc Res*. 2020;116(2):339-352. doi:10.1093/cvr/cvz119
19. Trevino MB, Machida Y, Hallinger DR, et al. Perilipin 5 regulates islet lipid metabolism and insulin secretion in a cAMP-dependent manner: implication of its role in the postprandial insulin secretion. *Diabetes*. 2015;64(4):1299-1310. doi:10.2337/db14-0559
20. Scorletti E, Carr RM. A new perspective on NAFLD: focusing on lipid droplets. *J Hepatol*. 2022;76(4):934-945. doi:10.1016/j.jhep.2021.11.009
21. Zhu Y, Ren C, Zhang M, Zhong Y. Perilipin 5 reduces oxidative damage associated with lipotoxicity by activating the PI3K/ERK-mediated Nrf2-ARE signaling pathway in INS-1 pancreatic β-cells. *Front Endocrinol (Lausanne)*. 2020;11:166. doi:10.3389/fendo.2020.00166
22. Lin J, Chen A. Perilipin 5 restores the formation of lipid droplets in activated hepatic stellate cells and inhibits their activation. *Lab Invest*. 2016;96(7):791-806. doi:10.1038/labinvest.2016.53
23. Tetri LH, Basaranoglu M, Brunt EM, Yerian LM, Neuschwander-Tetri BA. Severe NAFLD with hepatic necroinflammatory changes in mice fed trans fats and a high-fructose corn syrup equivalent. *Am J Physiol Gastrointest Liver Physiol*. 2008;295(5):G987-G995. doi:10.1152/ajpgi.90272.2008
24. Mederacke I, Dapito DH, Affò S, Uchinami H, Schwabe RF. High-yield and high-purity isolation of hepatic stellate cells from normal and fibrotic mouse livers. *Nat Protoc*. 2015;10(2):305-315. doi:10.1038/nprot.2015.017
25. Feng Y, Nie L, Thakur MD, et al. A multifunctional lentiviral-based gene knockdown with concurrent rescue that controls for off-target effects of RNAi. *Genomics Proteomics Bioinformatics*. 2010;8(4):238-245. doi:10.1016/s1672-0229(10)60025-3
26. Fraley SI, Feng Y, Krishnamurthy R, et al. A distinctive role for focal adhesion proteins in three-dimensional cell motility. *Nat Cell Biol*. 2010;12(6):598-604. doi:10.1038/ncb2062
27. Mashek DG. Hepatic lipid droplets: a balancing act between energy storage and metabolic dysfunction in NAFLD. *Mol Metab*. 2021;50:101115. doi:10.1016/j.molmet.2020.101115
28. Nagata S. Apoptosis and clearance of apoptotic cells. *Annu Rev Immunol*. 2018;36:489-517. doi:10.1146/annurev-immunol-042617-053010
29. Du D, Liu C, Qin M, et al. Metabolic dysregulation and emerging therapeutical targets for hepatocellular carcinoma. *Acta Pharm Sin B*. 2022;12(2):558-580. doi:10.1016/j.apsb.2021.09.019
30. Li H, Zhou Y, Wang H, et al. Crosstalk between liver macrophages and surrounding cells in nonalcoholic steatohepatitis. *Front Immunol*. 2020;11:1169. doi:10.3389/fimmu.2020.01169
31. Khomich O, Ivanov AV, Bartosch B. Metabolic hallmarks of hepatic stellate cells in liver fibrosis. *Cell*. 2019;9(1):24. doi:10.3390/cells9010024
32. Trivedi P, Wang S, Friedman SL. The power of plasticity-metabolic regulation of hepatic stellate cells. *Cell Metab*. 2021;33(2):242-257. doi:10.1016/j.cmet.2020.10.026
33. Mass Sanchez PB, Krizanac M, Weiskirchen R, Asimakopoulos A. Understanding the role of perilipin 5 in non-alcoholic fatty liver disease and its role in hepatocellular carcinoma: a review of novel insights. *Int J Mol Sci*. 2021;22(10):5284. doi:10.3390/ijms22105284
34. Lin SC, Hardie DG. AMPK: sensing glucose as well as cellular energy status. *Cell Metab*. 2018;27(2):299-313. doi:10.1016/j.cmet.2017.10.009
35. Li Z, Ding Q, Ling LP, et al. Metformin attenuates motility, contraction, and fibrogenic response of hepatic stellate cells in vivo and in vitro by activating AMP-activated protein kinase. *World J Gastroenterol*. 2018;24(7):819-832. doi:10.3748/wjg.v24.i7.819
36. Jain MR, Giri SR, Bhoi B, et al. Dual PPARα/γ agonist saroglitazar improves liver histopathology and biochemistry in experimental NASH models. *Liver Int*. 2018;38(6):1084-1094. doi:10.1111/liv.13634
37. Hur W, Kang BY, Kim SM, et al. Serine protease HtrA2/Omi deficiency impairs mitochondrial homeostasis and promotes hepatic Fibrogenesis via activation of hepatic stellate cells. *Cell*. 2019;8(10):1119. doi:10.3390/cells8101119
38. Zhao Y, Wang Z, Feng D, et al. p66Shc contributes to liver fibrosis through the regulation of mitochondrial reactive oxygen species. *Theranostics*. 2019;9(5):1510-1522. doi:10.7150/thno.29620
39. Ahmed ST, Craven L, Russell OM, Turnbull DM, Vincent AE. Diagnosis and treatment of mitochondrial myopathies. *Neurotherapeutics*. 2018;15(4):943-953. doi:10.1007/s13311-018-00674-4
40. Chiang JL, Shukla P, Pagidas K, et al. Mitochondria in ovarian aging and reproductive longevity. *Ageing Res Rev*. 2020;63:101168. doi:10.1016/j.arr.2020.101168
41. Roosterman D, Cottrell GS. Rethinking the citric acid cycle: connecting pyruvate carboxylase and citrate synthase to the flow of energy and material. *Int J Mol Sci*. 2021;22(2):604. doi:10.3390/ijms22020604
42. Marí M, de Gregorio E, de Dios C, et al. Mitochondrial glutathione: recent insights and role in disease. *Antioxidants (Basel)*. 2020;9(10):909. doi:10.3390/antiox9100909
43. Schaupp CM, Botta D, White CC, et al. Persistence of improved glucose homeostasis in Gclm null mice with age and cadmium treatment. *Redox Biol*. 2022;49:102213. doi:10.1016/j.redox.2021.102213
44. Espinosa-Díez C, Miguel V, Vallejo S, et al. Role of glutathione biosynthesis in endothelial dysfunction and fibrosis. *Redox Biol*. 2018;14:88-99. doi:10.1016/j.redox.2017.08.019
45. Dong GQ, Calhoun S, Fan H, et al. Prediction of substrates for glutathione transferases by covalent docking. *J Chem Inf Model*. 2014;54(6):1687-1699. doi:10.1021/ci5001554
46. Raggi C, Taddei ML, Sacco E, et al. Mitochondrial oxidative metabolism contributes to a cancer stem cell phenotype in cholangiocarcinoma. *J Hepatol*. 2021;74(6):1373-1385. doi:10.1016/j.jhep.2020.12.031
47. Dusabimana T, Park EJ, Je J, et al. P2Y2R deficiency ameliorates hepatic steatosis by reducing lipogenesis and enhancing fatty acid β-oxidation through AMPK and PGC-1α induction in high-fat diet-fed mice. *Int J Mol Sci*. 2021;22(11):5528. doi:10.3390/ijms22115528
48. MacParland SA, Liu JC, Ma XZ, et al. Single cell RNA sequencing of human liver reveals distinct intrahepatic macrophage populations. *Nat Commun*. 2018;9(1):4383. doi:10.1038/s41467-018-06318-7
49. Cubero FJ. Shutting off inflammation: a novel switch on hepatic stellate cells. *Hepatology*. 2016;63(4):1086-1089. doi:10.1002/hep.28442

SUPPORTING INFORMATION

Additional supporting information can be found online in the Supporting Information section at the end of this article.

How to cite this article: Yin X, Dong L, Wang X, et al. Perilipin 5 regulates hepatic stellate cell activation and high-fat diet-induced non-alcoholic fatty liver disease. *Anim Models Exp Med*. 2024;7:166-178. doi:10.1002/ame2.12327